INSTITUTE OF PHYSICS PUBLISHING SUPERCONDUCTOR SCIENCE AND TECHNOLOGY

Supercond. Sci. Technol. **18** (2005) 158–165 doi:10.1088/0953-2048/18/1/025

Generated heat during pulse field magnetizing for REBaCuO (RE = Gd, Sm, Y) bulk superconductors with different pinning abilities

Hiroyuki Fujishiro[1], Masahiko Kaneyama[1], Kazuya Yokoyama[2], Tetsuo Oka[2] and Koshichi Noto[2]

[1] Faculty of Engineering, Iwate University, 4-3-5 Ueda, Morioka 020-8551, Japan
[2] Iwate Industrial Promotion Center, 3-52-2, Iioka-shinden, Morioka 020-0852, Japan

E-mail: fujishiro@iwate-u.ac.jp

Received 24 May 2004, in final form 3 September 2004
Published 23 November 2004
Online at stacks.iop.org/SUST/18/158

Abstract

Pulse field magnetizing (PFM) using five successive magnetic pulses (Nos 1–5) with the same amplitude from 3.01 to 5.42 T has been performed for three types of cryo-cooled REBaCuO bulk superconductor discs (RE = Gd, Sm, Y) with an identical size. The time evolution and spatial distribution of temperature $T(t)$, the total trapped magnetic flux Φ_T^P and the trapped magnetic field B_T^P have been measured after applying the magnetic pulse. The total magnetic flux Φ_T^{FC} trapped by the field cooled magnetizing (FCM) is the largest for the Gd bulk and is the smallest for the Y bulk. The time and position dependences of $T(t)$ during PFM show a characteristic behaviour depending on the species of bulks which results from the difference in the strength of the pinning force F_p. The generated heat $Q(\text{No } i)$ after the No i pulse has been estimated based on the maximum temperature rise ΔT_{max} and the specific heat C. The $\Delta Q = Q(\text{No } 1)–Q(\text{No } 5)$ value, which is mainly contributed by the pinning power loss (Q_p) for pulse No 1, is the smallest for the Y bulk, and the $Q(\text{No } 5)$ value, which is mainly contributed by the viscous flow loss (Q_v), is the smallest for the Gd bulk. These results suggest that the heat generation by PFM is closely related to the strength of F_p of the bulk crystal.

1. Introduction

As is well known, the critical current density J_c and the trapped magnetic field B_T of REBaCuO bulk superconductors (RE: rare earth element) are determined by the species of the RE element and the content, the particle size and the dispersion of the RE_2BaCuO_5 non-superconducting phase acting as a pinning centre for the magnetic fluxes [1]. The B_T value or the total trapped magnetic flux Φ_T of the bulks has been enhanced by the improvement of the fabrication processes [2, 3]. For practical applications of the bulk superconductors as a strong bulk magnet for the magnetic separation, magnetic levitation and so on [4, 5], it is important to improve the mechanical and thermal properties besides J_c and B_T. Tomita *et al* [6] realized the trapped magnetic field of 17.24 T at 29 K in a YBaCuO bulk by field cooled magnetizing (FCM) from 17.9 T to zero. They used two key technologies; one is the mechanical reinforcement by resin impregnation, and the other is the thermal conduction enhancement by impregnating the highly thermally conductive alloy into the small drilled hole. In addition to the FCM method, pulse field magnetizing (PFM) has been recently investigated and developed in order to strongly magnetize the bulk superconductors [7]. Mizutani's group proposed a novel PFM method of iterative magnetizing operations with gradually reducing amplitudes, named the IMRA method [8, 9]. It was demonstrated that, by the IMRA

method, the YBaCuO bulk could trap almost the same amount of the magnetic flux as the FCM method in liquid nitrogen [7]. At temperatures lower than 77 K, however, the maximum value of B_T and Φ_T by PFM including the IMRA method is generally lower than that by FCM as reported for the SmBaCuO bulk superconductors with the stronger pinning force F_p [8, 9]. A possible reason may be a large temperature rise caused by the magnetization hysteresis loss and by the viscous loss due to the magnetic flux motion in a short pulse field period, which results in the decrease of B_T. The realization of the trapped magnetic field by PFM below 77 K ranking with FCM is greatly desired because the cryo-cooled refrigerator is now very popular to cool bulk superconductors instead of liquid nitrogen.

We have studied the time evolution and spatial distribution of the temperature rise $\Delta T(t)$ at the surface of the cryo-cooled YBaCuO [10] and SmBaCuO [11, 12] bulk superconductors after PFM. The $\Delta T(t)$ behaviour changed depending on the initial stage temperature T_s, the applied pulse field B_{ex} and the distribution of B_T before applying the pulse field. The measurement on the spatial distribution of $\Delta T(t)$ enabled us to locate the easy path through which the fluxes preferentially intrude into the bulk. We have estimated the generated heat Q during PFM using ΔT and the specific heat C [13].

The bulk superconductors with a stronger F_p generally result in a higher J_c and consequently show a higher B_T. The bulks with a higher B_T are expected to show a larger pinning loss Q_p. The temperature measurements and the Q estimation during PFM for the bulk superconductors with various B_T and J_c characteristics give us valuable information for pinning power loss Q_p and the viscous flow loss Q_v. In this paper, we report the time and position dependences of $\Delta T(t)$, the trapped field B_T^P and the trapped magnetic flux Φ_T^P after applying the five successive pulse fields (No 1–No 5) ranging from $B_{ex} = 3.01$ to 5.42 T for the cryo-cooled REBaCuO bulk superconductors (RE = Gd, Sm, Y). From the measured maximum temperature rise ΔT_{max} and the specific heat C for each bulk, the generated heat Q is calculated and the contribution of Q_p and Q_v to the total Q are discussed. We also discuss the relation between Φ_T^P and the heat generation.

2. Experimental details

Three types of highly c-axis oriented REBaCuO bulk superconductor discs on a commercial base were used in this study, which had the same size, 45 mm in diameter and 15 mm in thickness. The GdBaCuO bulk, fabricated by Nippon Steel Corporation Ltd, is composed of $GdBa_2Cu_3O_y$ (Gd123) and Gd_2BaCuO_5 (Gd211) with the molar ratio of Gd123:Gd211 = 1.0:0.4, 10.0 wt% Ag_2O powder and 0.5 wt% Pt powder. Hereafter, we abbreviate this bulk as the Gd bulk. The SmBaCuO bulk (Sm bulk), fabricated by Dowa Mining Co., Ltd, is composed of $SmBa_2Cu_3O_y$ (Sm123) and Sm_2BaCuO_5 (Sm211) with the molar ratio of Sm123:Sm211 = 1.0:0.3, 15.0% Ag_2O powder and 0.42 wt% Pt powder. The YBaCuO bulk (Y bulk), fabricated by Dowa Mining Co., Ltd, is composed of $YBa_2Cu_3O_y$ (Y123) and Y_2BaCuO_5 (Y211) with the molar ratio of Y123:Y211 = 1.0:0.4, 15.0 wt% Ag_2O powder and 0.42 wt% Pt powder. These bulks were uniformly impregnated by epoxy resin in vacuum. The epoxy resin layers on both upper and lower sides of the bulk were removed in order to measure the precise temperature on the bulk surface and to reduce the thermal contact resistance between the bulk and the cold stage. Figure 1(a) shows the positions for the temperature measurement on the bulk, which was tightly stuck on the sapphire plate (45 mm in diameter and 20 mm in thickness) attached to the cold stage of a Gifford McMahon (GM) cycle helium refrigerator (AISIN, GR103) using indium foil and was evacuated below $\simeq 10^{-5}$ Torr. The temperature rise due to the eddy current in the Cu cold stage was reduced by the inserted sapphire plate between the stage and the sample and was confirmed to be below 0.2 K at 100 K ($> T_c$) for 5 T pulse field. The initial stage temperature T_s was fixed at 40 K. The temperatures $T0$ at the centre of the bulk (P0) and $T1$–$T4$ at P1–P4 in the four growth sector regions (GSRs) were measured by chromel–constantan thermocouples (76 μm in diameter) adhered to the bulk surface using GE7031 varnish. P1–P4 were situated on the central lines of each GSR, 9 mm apart from P0. Each temperature was measured about 7 times s^{-1} just after applying the pulse field.

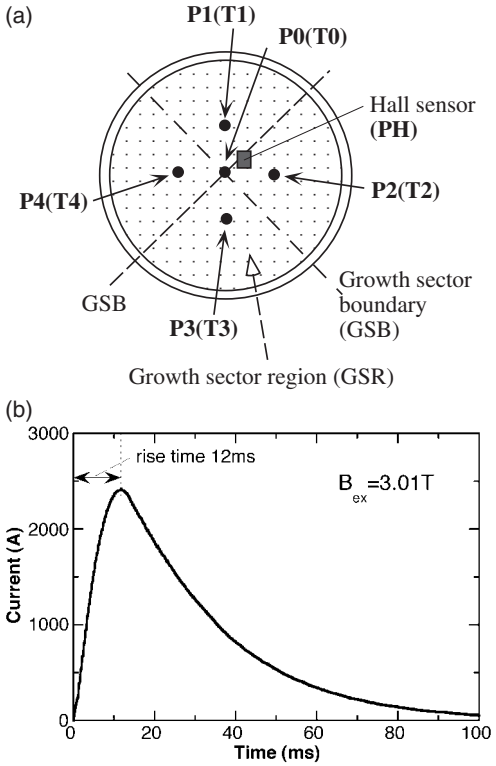

Figure 1. (a) The positions for the temperature and trapped field measurements on the surface of the REBaCuO bulk disc with the same size (45 mm in diameter, 15 mm in thickness). P0–P4 for the temperature measurements of $T0$–$T4$ are indicated. The trapped field B_T on the bulk surface is measured using an adhered Hall sensor at PH. (b) An example of the time dependence of the pulse current $I(t)$ which flows through the pulse coil for $B_{ex} = 3.01$ T.

The bulk crystals were magnetized using a pulse coil ($L = 1.08$ mH) dipped in liquid N_2. Figure 1(b) shows an example of the time dependence of the pulse current $I(t)$ which flows through the pulse coil for $B_{ex} = 3.01$ T. The rise time of the pulse field was about 12 ms. The strength of the pulse field $B_{ex}(t)$ was calculated from $I(t)$, which ranged from 3.01 to 5.42 T. The field shielding effect due to the Cu cold

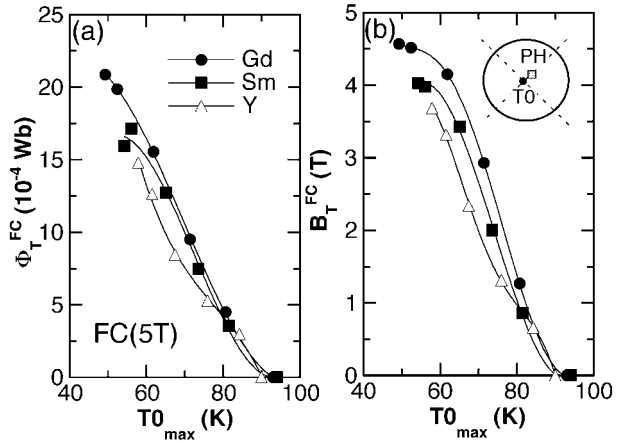

Figure 2. (a) The trapped total magnetic flux Φ_T^{FC} and (b) the trapped field B_T^{FC} by field cooled magnetizing (FCM) for the REBaCuO bulks (RE = Gd, Sm, Y) as a function of the maximum temperature at the bulk centre ($T0_{max}$).

stage is not important because of the rather large pulse rising time and the inserted sapphire spacer. The trapped magnetic field B_T^P just on the bulk was measured by the Hall sensor (F W Bell, model BHA 921) adhered to position PH with a 2.5 mm distance from P0 as shown in figure 1(a). The total trapped magnetic flux Φ_T^P and the distribution of the trapped magnetic flux density $B_T^{3\ mm}$ was measured using an axial type Hall sensor, which scanned 3 mm above the bulk surface stepwise with a pitch of 1.2 mm. Five magnetic pulses with the same amplitude B_{ex} were applied sequentially and $T(t)$, B_T^P and Φ_T^P were measured at each stage. Hereafter we abbreviate the five pulses as No 1–No 5. The temperature rise after applying the pulse field was recovered to the initial temperature ($T_s = 40$ K) for 15–20 min. The trapped field B_T^{FC} and the trapped magnetic flux Φ_T^{FC} by FCM were also measured at several temperatures using the cryo-cooled superconducting magnet in order to elucidate the maximum ability of flux trapping for each bulk. During FCM, the static magnetic field of 5 T was decreased to 0 T in 18 min (0.278 T min^{-1}). The temperature dependence of the specific heat $C(T)$ was estimated by the thermal conductivity κ divided by the thermal diffusivity α measured for parallelepiped samples with the same composition as the bulk discs.

3. Results and discussion

3.1. Trapped magnetic flux Φ_T^{FC} and trapped field B_T^{FC} by FCM

Figures 2(a) and (b) show the trapped total magnetic flux Φ_T^{FC} and the trapped field B_T^{FC} by FCM for each bulk, respectively, as a function of the maximum temperature $T0_{max}$ at the centre (P0) of the bulk. The Φ_T^{FC} and B_T^{FC} values increase with decreasing temperature for all the bulks. Below 80 K, Φ_T^{FC} and B_T^{FC} are the largest for the Gd bulk and become smaller for Sm bulk and Y bulk in this order. The differences in Φ_T^{FC} and B_T^{FC} for the three bulks should result from the difference in the J_c and F_p values. The temperature rise $\Delta T0^{FC}$ during the FCM process is about 2–4 K at $T0_{max} \simeq 50$ K for the field decreasing rate of 0.278 T min^{-1} and decreases with increasing $T0_{max}$. $\Delta T0^{FC}$ of the Gd bulk is the smallest and that of the Sm bulk is the largest around 50 K. $\Delta T0^{FC}$ increased and B_T^{FC} decreased with the increase in the field decreasing rate as was described elsewhere [14]. For these three bulk discs with a different F_p, the time evolution of the temperatures $T0(t)$–$T4(t)$, trapped magnetic flux Φ_T^P and trapped field B_T^P have been measured after PFM as shown in the following subsection.

3.2. Temperature rise and trapped magnetic flux for Gd, Sm and Y bulks by PFM

Figures 3(a) and (b) show the time evolutions of $T0(t)$–$T4(t)$ for the Y bulk at $B_s = 40$ K after applying the No 1 and No 5 pulse fields of 3.01 and 3.87 T, respectively. Figures 3(c) and (d) show the similar temperature changes for the Sm bulk and figures 3(e) and (f) show those for the Gd bulk. The inset for each figure shows the distribution of the trapped magnetic flux density $B_T^{3\ mm}$ after applying pulse No 1. It can clearly be seen that the absolute value and the time evolution of temperatures $T0(t)$–$T4(t)$ for pulse No 1 depends on the species of the bulk. In figure 3(a) for the Y bulk, $T4(t)$ and $T1(t)$ rise first with $\Delta T_{max} \simeq 8$ K, followed by $T2(t)$, $T0(t)$ and $T3(t)$ in this order for $B_{ex} = 3.01$ T, which suggests that F_p in GSR4 and GSR1 is relatively weak. Since the time profile of $T0$–$T4$ is smooth and does not show a clear peak, the position dependence of F_p may be small. The spatial dependence of the maximum temperature rise ΔT_{max} is also small. The applied field of $B_{ex} = 3.01$ T is high enough to destroy the pinning potential barrier in the peripheral region. But the magnetic flux does not reach the centre of the bulk sufficiently as shown in the distribution of $B_T^{3\ mm}$. For $B_{ex} = 3.87$ T in figure 3(b), the temperature rise increases ($\Delta T_{max} \simeq 18$ K) and the time profile of $T2(t)$, $T0(t)$ and $T3(t)$ becomes nearly identical. The $B_T^{3\ mm}$ profile indicates that the flux penetrates into the bulk uniformly.

In figures 3(c) and (d) for the Sm bulk, on the other hand, the time profile of temperature shows a large and clear peak in some GSRs. $T2(t)$ and $T3(t)$ rise first with a sharp peak ($\Delta T_{max} \simeq 16$ K), followed by $T4(t)$ and $T1(t)$, and $T0(t)$ rise latest for pulse No 1, and then the temperatures approach the initial temperature. The magnetic fluxes should penetrate into the bulk crystal preferentially through the weaker pinning regions. The magnetic flux easily intrudes into the Sm bulk through the regions around P2 and P3, and the temperature rise ΔT is more intense in these GSRs. The trapped field $B_T^{3\ mm}$ is also enhanced around P2 and P3. For $B_{ex} = 3.87$ T shown in figure 3(d), the temperature rises increase (e.g., $\Delta T_{max} \simeq 26$ K at $T3$). The $B_T^{3\ mm}$ value increases and the $B_T^{3\ mm}$ profile takes a cone shape. In figures 3(e) and (f) for the Gd bulk, the temperature rises do not take place uniformly after pulse No 1, similarly to the Sm bulk; the temperature rise is the largest at $T3$ ($\Delta T_{max} \simeq 10$ K) for $B_{ex} = 3.01$ T and at $T1$ ($\Delta T_{max} \simeq 24$ K) for $B_{ex} = 3.87$ T where F_p may be relatively small. In this way, the characteristic temperature rises can be seen to depend on the species of the bulk crystal. For the pulse field applications from No 2 to No 5 for each B_{ex}, the characteristic peak in $T(t)$ of the Gd and Sm bulks is completely wiped out and ΔT decreases and then saturates. In all cases of flux penetration, $T0(t)$ at the centre of the bulk rises last because the heat is mainly generated in the peripheral

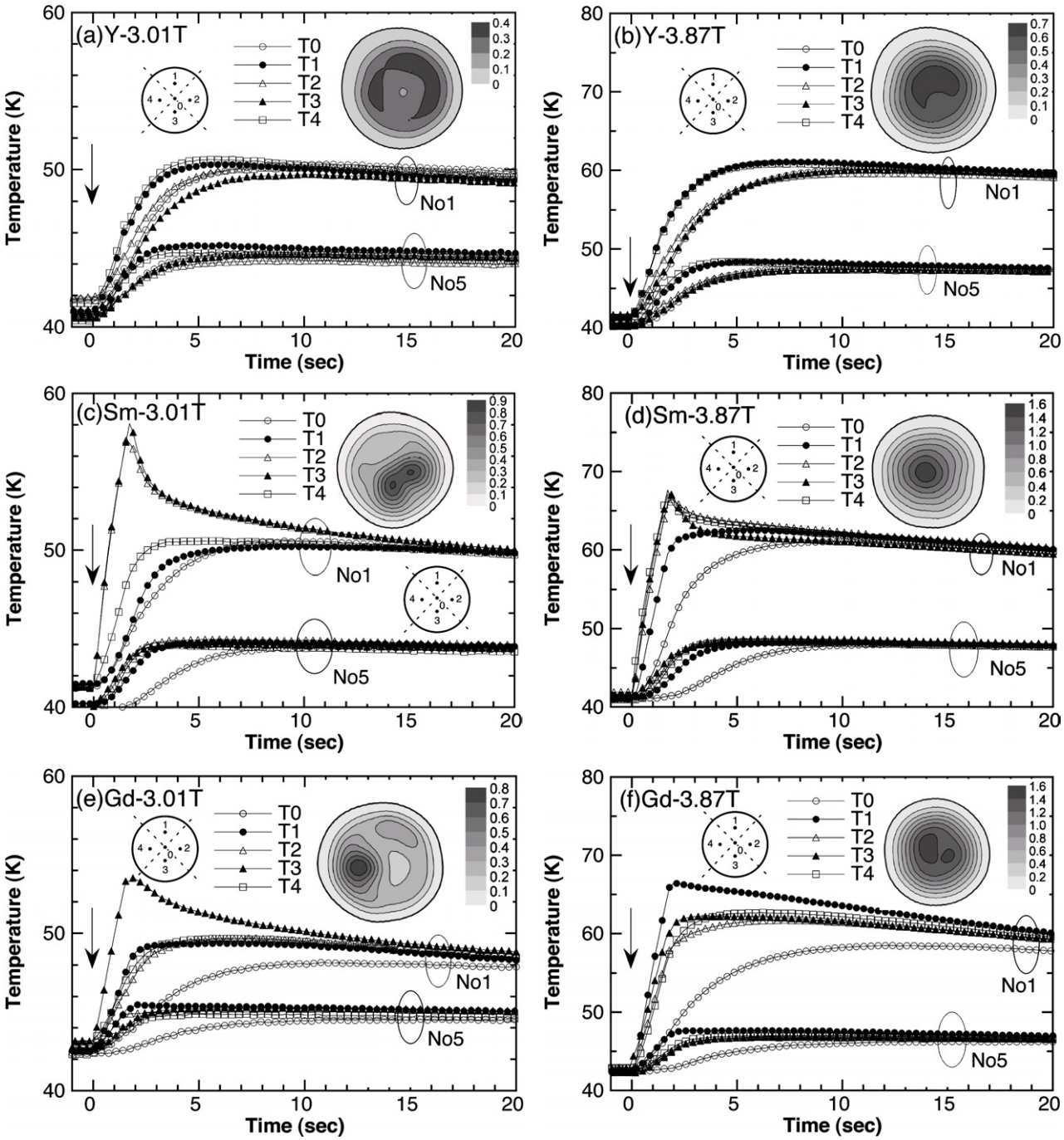

Figure 3. The time evolutions of temperatures $T0(t)$–$T4(t)$ at $T_s = 40$ K after applying the No 1 and No 5 pulse fields of (a) 3.01 T and (b) 3.87 T for the Y bulk. (c) and (d) show similar results for the Sm bulk, and (e) and (f) for the Gd bulk. The inset for each figure shows the distribution of the trapped magnetic flux density $B_T^{3\ mm}$ after applying pulse No 1.

region where the flux moves faster and the generated heat diffuses toward the central region.

Figures 4(a) shows the pulse number dependence of the average temperature rise ΔT for each bulk after applying the pulse field B_{ex} (=3.01–4.64 T). ΔT is defined by the averaged value of the temperature rises of $T1$–$T4$ and the bar shows the maximum and minimum temperature rise of $\Delta T1$–$\Delta T4$. In all the cases, ΔT monotonically decreases and approaches a steady value with increasing pulse number. ΔT of the Sm bulk is the largest for each pulse number and for each B_{ex}. The ΔT values of the Y bulk after pulse No 1 are smaller than those of the Sm bulk but are similar to the Sm bulk after pulse No 2. On the other hand, for the Gd bulk, ΔT is the smallest for each B_{ex}. Since the temperature rise occurs under the nearly adiabatic condition in the PFM process, the thermal contact resistance between the bulk disc and the cold stage of a GM refrigerator hardly influences the maximum temperature rise ΔT_{max} [10]. Figure 4(b) shows the pulse number dependence of the difference of the temperature rise $dT = \Delta T(n-1) - \Delta T(n)$ between the ΔT after the $(n-1)$th

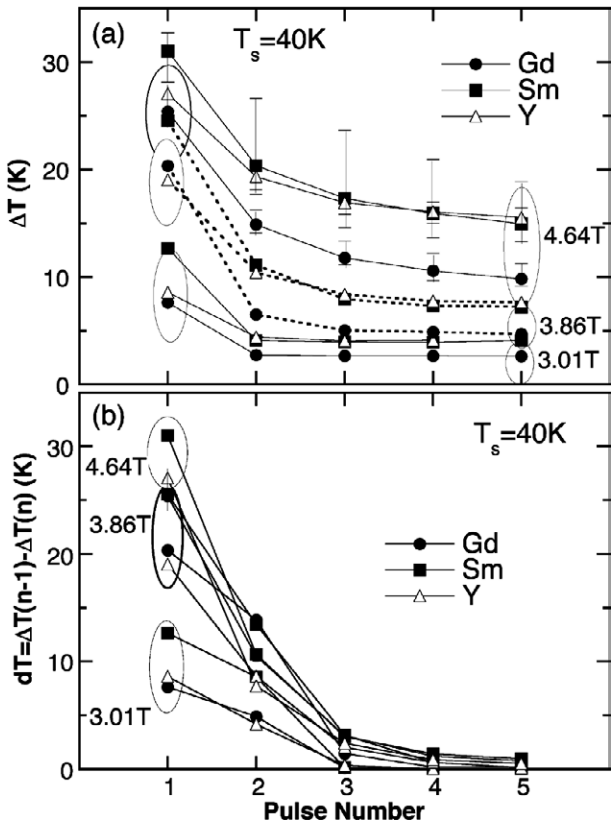

Figure 4. The pulse number dependence of (a) the average temperature rise ΔT and (b) the difference of the temperature rise dT between the ΔT after the $(n-1)$th and (n)th pulses.

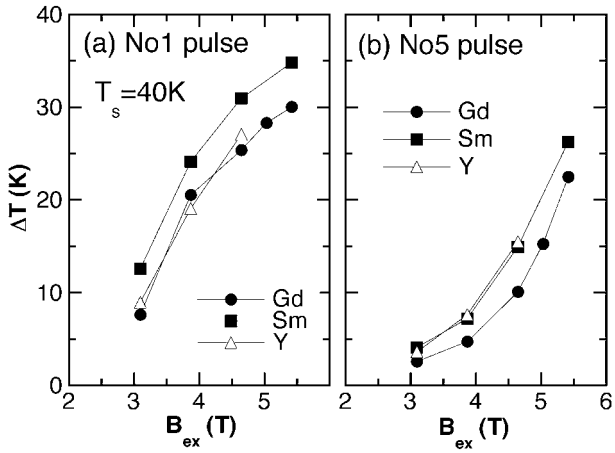

Figure 5. The average temperature rise ΔT of three bulks as a function of the applied field B_{ex} for pulses (a) No 1 and (b) No 5, respectively.

and that after the (n)th pulses. The dT value drastically reduces with the increase in the pulse number and then approaches zero.

Figures 5(a) and (b) show the average ΔT of three bulk discs as a function of B_{ex} for pulses No 1 and No 5, respectively. In both figures, ΔT increases with increasing B_{ex}. However, the ΔT–B_{ex} curves for pulse No 1 are convex and those for pulse No 5 are concave. The ΔT value of the Sm bulk is the largest for pulse No 1 and that of the Gd bulk is the smallest for pulse No 5.

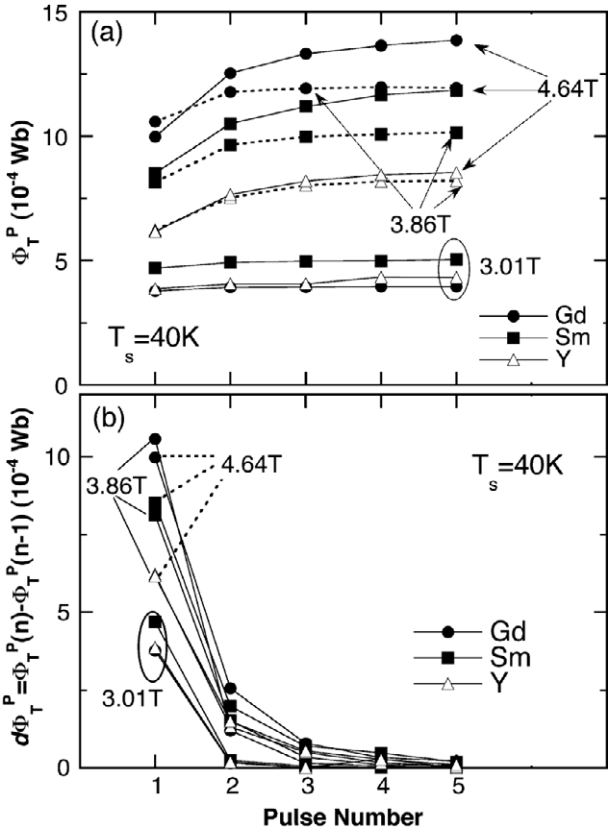

Figure 6. The pulse number dependence of (a) the total trapped magnetic flux Φ_T^P and (b) the increment of the trapped flux dΦ_T^P after the preceding pulse.

Figure 6(a) shows the pulse number dependence of the total trapped magnetic flux Φ_T^P of the three bulks for B_{ex} = 3.01–4.64 T. The largest amount of the fluxes is trapped during application of pulse No 1 to the virgin state bulks. Φ_T^P is gradually enhanced with increasing pulse number, approaching a fixed ultimate value for pulses No 4 and No 5. The increment of the trapped flux dΦ_T^P $(=\Phi_T^P(n)-\Phi_T^P(n-1))$ after the preceding pulse is presented in figure 6(b). The intrusion and additional trap of the magnetic flux are reduced by the presence of the already trapped flux. These saturation tendencies much resemble the behaviours of dT shown in figure 4(b). In figure 6(a), the Φ_T^P value for B_{ex} = 3.01 T is the largest for the Sm bulk and the smallest for the Gd bulk. For the Gd bulk, the pressure of the magnetic flux associated with a lower field cannot overcome the pinning potential barrier in the close vicinity of the surface region and the flux intrusion is impeded by the surface pinning barrier. On the other hand, for the applied fields of 3.86 and 4.64 T, the Φ_T^P value is the largest for Gd bulk and is the smallest for Y bulk. This trend is consistent with Φ_T^{FC} by FCM as shown in figure 2(a) and reflects the intrinsic pinning ability of each bulk.

Figures 7(a) and (b) show the trapped magnetic flux Φ_T^P after pulse No 1 and pulse No 5, respectively, as a function of B_{ex}. Φ_T^P increases with increasing B_{ex} for each bulk, shows a maximum and then decreases for B_{ex} higher than 4.64 T. These tendencies can be understood on the basis of the Φ_T^{FC}–$T0_{max}$ line as shown in figure 2(a) [10, 11]. When the pulse field B_{ex} higher than 4.64 T is applied to the bulk at T_s = 40 K,

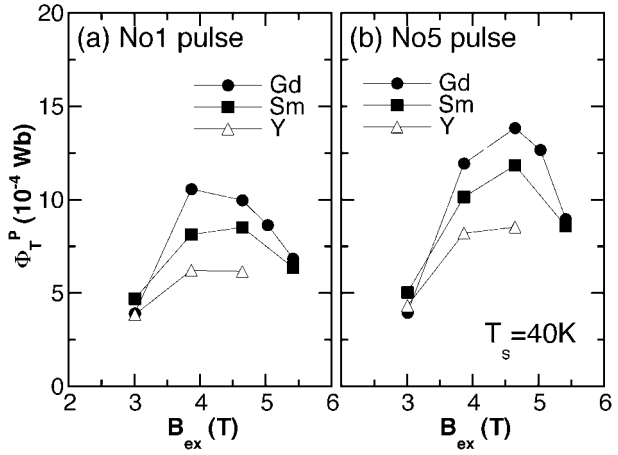

Figure 7. The total trapped magnetic flux Φ_T^P after (a) pulse No 1 and (b) pulse No 5 as a function of B_{ex}.

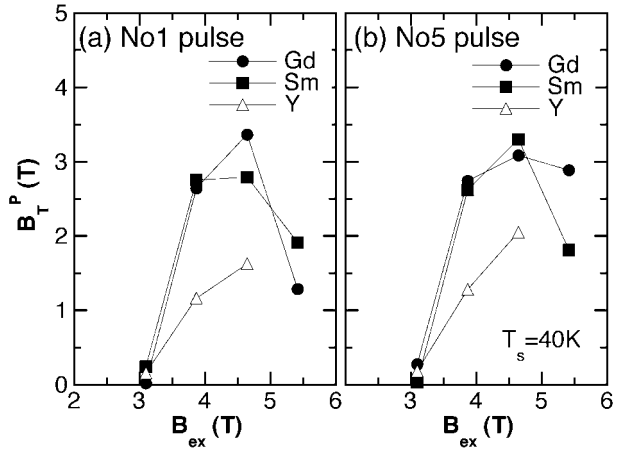

Figure 8. The trapped magnetic flux B_T^P at the position PH in figure 1 after (a) pulse No 1 and (b) pulse No 5 as a function of B_{ex}.

$T0_{max}$ of the bulk touches the Φ_T^{FC}–$T0_{max}$ line owing to the larger temperature rise and then Φ_T^{FC} decreases following the line. The larger temperature rise due to the violent flux motion weakens the pinning force F_p and hinders the flux trapping at this high level of B_{ex}. Figures 8(a) and (b) show the trapped magnetic field B_T^P for the application of pulse No 1 and pulse No 5, respectively, as a function of B_{ex}. Similarly to the Φ_T^P results, B_T^P shows a maximum around $B_{ex} = 4.64$ T for all bulks and then decreases with the further increase in B_{ex}. B_T^P of the Gd and Sm bulks is larger than that of the Y bulk. In all the bulks, B_T^P is very small for $B_{ex} = 3.01$ T. This result suggests that applied magnetic flux cannot reach the centre of the bulk but the trapped flux remains in the peripheral region as is seen in each inset in figure 3. It is worthwhile to note that the B_T^P value for the Gd bulk after the first (No 1) pulse application of 4.64 T is as high as about 3.40 T which is about 70% of the B_T^{FC} value in figure 2(b).

3.3. Specific heat of bulk superconductors

We have measured the thermal conductivity $\kappa(T)$ and the thermal diffusivity $\alpha(T)$ of the three types of parallelepiped samples with the same composition as the bulk discs. $\kappa(T)$

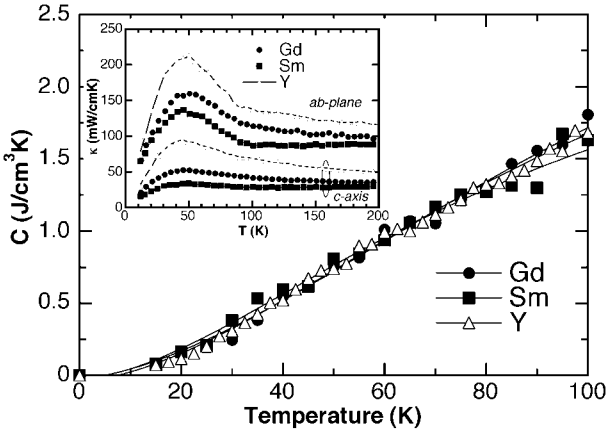

Figure 9. The temperature dependence of the estimated specific heat $C(T)$ for each bulk. The inset shows the ab-plane $\kappa_{ab}(T)$ and c-axis $\kappa_c(T)$ thermal conductivities of the three bulks.

was measured by a steady-state heat flow method between 10 and 300 K and the $\alpha(T)$ measurement was performed by an arbitrary heating method under an identical experimental set-up with the κ measurement [15]. The specific heat $C(T)$ (J cm^{-3} K^{-1}) was estimated from the relation $C = \kappa/\alpha$, which is presented in figure 9 for each bulk. The inset in figure 9 shows the temperature dependence of the thermal conductivity in the ab-plane (κ_{ab}) and along the c-axis (κ_c). The absolute values of $\kappa_{ab}(T)$ and $\kappa_c(T)$ are the largest for the Y bulk because of the higher Ag contents (=15 wt%) and, possibly, of the higher crystallinity compared with the Sm bulk, in which the phonon scattering by the crystal defect may be enhanced due to the Ba–Sm inter-diffusion [16]. The absolute values of $\alpha_{ab}(T)$ and $\alpha_c(T)$ were also the largest for the Y bulk and the smallest for the Sm bulk. As a result, the specific heat $C(T)$ of each bulk is almost identical irrespective of the RE element and somewhat different Ag content. Since the heat generation occurs under nearly an adiabatic condition during the PFM process, the $C(T)$ value should directly decide the temperature rise ΔT. The thermal conductivity of the bulk may affect the recovery time to the initial temperature and the temperature rise ΔT_{FC} in the FCM process.

3.4. Estimation of generated heat Q

The generated heat Q due to the pulse field application can be estimated using the following equation:

$$Q = \int_{T_s}^{T_s+\Delta T_{max}} C(T)V \, dT, \qquad (1)$$

where V is the volume of the bulk disc, T_s is the bulk initial temperature (= 40 K) and ΔT_{max} is the average maximum temperature rise. Figures 10(a) and (b) show the results of the Q(No 1) and Q(No 5) values after applying pulses No 1 and No 5, respectively, as a function of B_{ex}. Figure 10(c) shows the $\Delta Q = Q$(No 1)–Q(No 5) value as a function of B_{ex}. The heat generation Q during PFM can be regarded as the sum of the pinning loss Q_p and the viscous flow loss Q_v [12]. Similarly to ΔT in figure 4, the Φ_T^P values also almost saturate after pulse No 3 in figure 6. Accordingly, no additional flux trapping takes place during pulse No 5. Then Q(No 5) shown in figure 10(b)

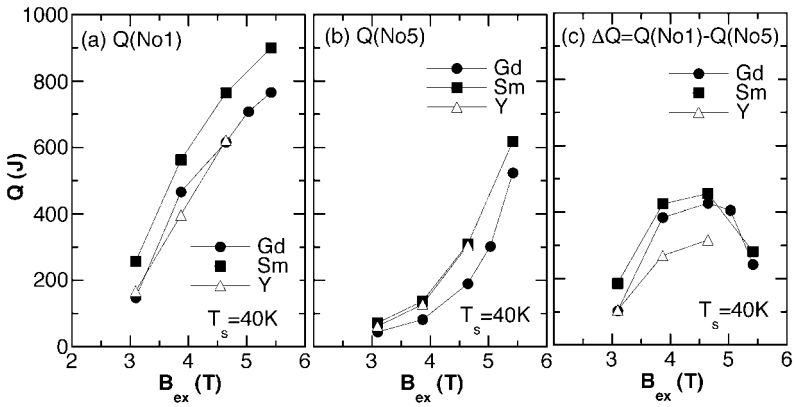

Figure 10. The estimated Q values as a function of B_{ex}. (a) The Q values after applying pulse No 1 (Q(No 1)), (b) the Q values after applying pulse No 5 (Q(No 5)) which are regarded as the sum of the pinning loss Q_p^s uncorrelated with the flux trapping and the viscous flow loss Q_v, (c) the $\Delta Q = Q$(No 1)$-Q$(No 5) values which stand for the heat generation for pulse No 1, directly connected to the flux trapping.

is given by the sum of the saturated hysteresis pinning power loss Q_p^s, which is not related to the flux trapping, and the viscous flow loss Q_v. Then the ΔQ value can be regarded as the heat generation due to the flux trapping during the pulse No 1 field, if we assume that the Q_v and Q_p^s values are not much different for each pulse. It can be clearly seen that the ΔQ value for the Y bulk is smaller than that for the Gd and Sm bulks which may result from the smallest F_p in the three bulks.

Though the Φ_T^P value of the Gd bulk shown in figure 7 is larger than that of the Sm bulk due to the stronger F_p, ΔQ of the Gd bulk is slightly smaller than that of the Sm bulk. As we can see in figures 3(c) and (d), $T2(t)$ and $T3(t)$ of the present Sm bulk rise quite rapidly and exhibit clear overshoots. This unusual behaviour of $T2(t)$ and $T3(t)$ suggests that the flux penetrates more easily along the easy paths containing or very near the $T2$ and $T3$ measuring points. The flux penetration in a irregular manner and the rampant flux motion along the easy paths may cause additional viscous loss Q_v in this Sm bulk. In figure 10(c), the ΔQ value takes a maximum at 4.64 T and decreases with the further increase in B_{ex}. ΔQ and the trapped magnetic flux Φ_T^P in figure 7(a) have very similar B_{ex} dependence; i.e., if ΔQ is large, Φ_T^P is also large. These results support our assumption that ΔQ can be roughly regarded as the heat generation correlated to the flux trapping. In figure 10(b), Q(No 5) is the smallest for the Gd bulk. The Gd bulk with the strongest F_p should trap the magnetic fluxes more intensely. In materials with stronger flux pinning centres, the flux motion is more strongly impeded. Then the viscous flow may be reduced, reducing the viscous flow loss as well.

The analyses of the magnetic and heat-loss behaviour of the bulk superconductor are desired to be performed quantitatively, applying the Bean critical state model. The Bean model describes the behaviour of the magnetic flux ϕ_T but does not directly deal with the heat-loss. In this study, we only measured the trapped flux Φ_T^P and the trapped field B_T^P after the pulse field application and the discussion cannot but remain phenomenological. Simultaneous measurements of the magnetization $M(t)$ during the pulse field and the temperature $T(t)$ are in progress and will be reported in a near future together with more quantitative analyses.

4. Summary

The time evolution and the spatial distribution of temperatures $T(t)$ for three types of REBaCuO bulk superconductors (RE = Gd, Sm, Y) with different flux pinning abilities have been measured after five iterative pulse fields (Nos 1–5) with the same amplitude (B_{ex} = 3.01–5.42 T). The generated heat Q has been estimated using the measured specific heat $C(T)$ and the maximum temperature rise ΔT_{max}. The relations between the temperature rise $\Delta T(t)$, the trapped magnetic flux Φ_T^P and the generated heat Q during pulse field magnetizing (PFM) have been investigated. Important experimental results and conclusions obtained in this study are summarized as follows.

(1) The trapped magnetic flux Φ_T^{FC} and the trapped field B_T^{FC} by the field cooled magnetizing (FCM) for the three bulk discs with the same size are the largest for the GdBaCuO bulk (Gd bulk) and the smallest for the YBaCuO bulk (Y bulk) below 80 K. Φ_T^{FC} and B_T^{FC} correspond to the maximum ability for the flux trapping in each bulk superconductor. These results suggest that the pinning force F_p and the critical current density J_c are the largest for the Gd bulk and the smallest for the Y bulk. The SmBaCuO bulk (Sm bulk) has the intermediate ability for the flux trap among these three bulk superconductors.

(2) For the low pulse field application (B_{ex} = 3.01 T), the magnetic flux uniformly and easily intrudes into the Y bulk due to the lower F_p compared with the other two bulks. As a result, the temperature rise of the Y bulk takes place uniformly in the peripheral region of the bulk disc. On the other hand, for the Gd and Sm bulk discs with the stronger pinning ability, the surface barrier against the flux intrusion is partially destroyed at P2 and P3 for the Sm bulk and only at P1 for the Gd bulk, where the F_p value may be locally weaker and the larger temperature rise takes place.

(3) For the higher pulse field application ($B_{ex} \geqslant 3.87$ T), the pinning potential is widely destroyed in the surface region of all the three bulks and the temperature rise occurs almost uniformly due to the uniform intrusion of the flux.

(4) The temperature dependence of the specific heat $C(T)(=\kappa/\alpha)$ of each bulk has been estimated by the simultaneously measured thermal conductivity κ and the

thermal diffusivity α. The $C(T)$ values of the three bulks are nearly the same and almost independent of the RE element and the small difference of the Ag contents.

(5) The generated heat Q during PFM has been estimated using the $C(T)$ value and the maximum temperature rise ΔT_{max}. The $\Delta Q = Q(\text{No 1}) - Q(\text{No 5})$ value, the difference between the generated heat of the No 1 pulse and pulse No 5, is the smallest for the Y bulk. The ΔQ shows a similar B_{ex} dependence as that of the trapped magnetic flux Φ_T^P. These results suggest that the ΔQ value stands for the heat generation, directly connected to the flux trapping for pulse No 1.

(6) The $Q(\text{No 5})$ value, which is regarded as the sum of the pinning hysteresis loss Q_p^s uncorrelated with the flux trapping and the viscous flow loss Q_v, is the smallest for the Gd bulk with the strongest F_p. The stronger pinning force may impede the flow of the untrapped fluxes, reducing the viscous flow loss.

Acknowledgments

The valuable suggestions by Professor M Ikebe of Iwate University are gratefully acknowledged. This work is partially supported by the Japan Science and Technology Agency under the Joint Research Project for Regional Intensive in the Iwate Prefecture on development of practical applications of magnetic field technology for use in the region and in everyday living.

References

[1] Murakami M, Sakai N, Higuchi T and Yoo S I 1996 *Supercond. Sci. Technol.* **9** 1015
[2] Nariki S, Sakai N and Murakami M 2002 *Supercond. Sci. Technol.* **15** 235
[3] Muralidhar M, Koblischka M R and Murakami M 2001 *Supercond. Sci. Technol.* **14** 1349
[4] Oka T, Yokoyama K and Noto K 2004 *IEEE Appl. Supercond.* **14** 1058
[5] Sawamura M and Morita M 2002 *Supercond. Sci. Technol.* **15** 774
[6] Tomita M and Murakami M 2003 *Nature* **421** 517
[7] Mizutani U, Oka T, Itoh Y, Yanagi Y, Yoshikawa M and Ikuta H 1998 *Appl. Supercond.* **6** 235
[8] Ikuta H, Yanagi Y, Yoshikawa M, Itoh Y, Oka T and Mizutani U 2001 *Physica* C **357–360** 837
[9] Ishihara H, Ikuta H, Itoh Y, Yanagi Y, Yoshikawa M, Oka T and Mizutani U 2001 *Physica* C **357–360** 763
[10] Fujishiro H, Oka T, Yokoyama K and Noto K 2003 *Supercond. Sci. Technol.* **16** 809
[11] Fujishiro H, Oka T, Yokoyama K and Noto K 2004 *Supercond. Sci. Technol.* **17** 57
[12] Fujishiro H, Oka T, Yokoyama K, Kaneyama M and Noto K 2004 *IEEE Appl. Supercond.* **14** 1054
[13] Fujishiro H, Yokoyama K, Kaneyama M, Oka T and Noto K 2004 *Physica* C **412–414** 646
[14] Oka T, Yokoyama K, Kaneyama M, Fujishiro H and Noto K 2004 *Physica* C submitted
[15] Ikebe M, Fujishiro H, Naito T and Noto K 1994 *J. Phys. Soc. Japan* **63** 3107
[16] Fujishiro H and Kohayashi S 2002 *IEEE Trans. Appl. Supercond.* **12** 1124